Altered biventricular hemodynamic forces in patients with repaired tetralogy of Fallot and right ventricular volume overload because of pulmonary regurgitation

Sjöberg, Pia; Töger, Johannes; Hedström, Erik; Arvidsson, Per Martin; Heiberg, Einar; Arheden, Hakan; Gustafsson, Ronny; Nozohoor, Shahab; Carlsson, Marcus

Published in:
American Journal of Physiology - Heart and Circulatory Physiology

DOI:
10.1152/ajpheart.00330.2018

2018

Document Version:
Peer reviewed version (aka post-print)

Title page

Title

Altered biventricular hemodynamic forces in patients with repaired Tetralogy of Fallot and right ventricular volume overload due to pulmonary regurgitation

Authors

Pia Sjöberg[1], Johannes Töger[1,4], Erik Hedström[1,3], Per Arvidsson[1], Einar Heiberg[1,4], Håkan Arheden[1], Ronny Gustafsson[2], Shahab Nozohoor[2], Marcus Carlsson[1]

Affiliation

1: Lund University, Department of Clinical Sciences, Lund, Clinical Physiology, Skåne University Hospital, Sweden.

2: Lund University, Department of Clinical Sciences, Lund, Cardiothoracic Surgery, Skåne University Hospital, Sweden.

3: Lund University, Department of Clinical Sciences, Lund, Diagnostic Radiology, Skåne University Hospital, Sweden.

4: Lund University, Department of Biomedical Engineering, Faculty of Engineering, Sweden.

List of authors contributions

- MC and HA conceived the study.
- MC, RG, SN and PS designed the study.
- JT and EH developed the methodology.
- MC, PA, PS, RG and SN included patients and controls.
- PS, PA and MC performed the analysis.
- All authors interpreted the results and contributed with intellectual input to the manuscript and approved the final version.
-

Running Head

Hemodynamic forces in right ventricular volume overload

Address for Correspondence

Marcus Carlsson, Address: Dept of Clinical Physiology, Skåne University Hospital, 221 85 Lund, Sweden. Phone: +4646173989, e-mail: marcus.carlsson@med.lu.se

Abstract

Intracardiac hemodynamic forces have been proposed to influence remodeling and be a marker of ventricular dysfunction. We aimed to quantify the hemodynamic forces in repaired tetralogy of Fallot (rToF) patients to further understand the pathophysiological mechanisms as this could be a potential marker for pulmonary valve replacement (PVR) in these patients. Patients with rToF and PR>20% (n=18) and healthy controls (n=15) underwent magnetic resonance imaging (MRI)

including 4D-flow. A subset of patients (n=8) underwent PVR and MRI after surgery. Time-resolved hemodynamic forces were quantified using 4D-flow data and indexed to ventricular volume. Patients had higher systolic and diastolic left ventricular (LV) hemodynamic forces compared to controls in the lateral-septal/LVOT ($p=0.011$; $p=0.0031$) and inferior-anterior ($p<0.0001$; $p<0.0001$) directions, which are forces not aligned with blood flow. Forces did not change after PVR. Patients had higher RV diastolic forces compared to controls in the diaphragm-RVOT ($p<0.001$) and apical-basal ($p=0.0017$) directions. After PVR RV systolic forces in the diaphragm-RVOT direction decreased ($p=0.039$) to lower levels than in controls ($p=0.0064$). RV diastolic forces decreased in all directions ($p=0.0078$; $p=0.0078$; $p=0.039$) but were still higher than in controls in diaphragm-RVOT direction ($p=0.046$). In conclusion, patients with rToF and PR had LV hemodynamic forces less aligned with the intraventricular blood flow compared to controls and higher diastolic RV forces along the regurgitant flow direction in the RVOT and that of tricuspid inflow. Remaining force differences in LV and RV after PVR suggest that biventricular pumping does not normalize after surgery.

New & Noteworthy

Biventricular hemodynamic forces in patients with repaired Tetralogy of Fallot and pulmonary regurgitation were quantified for the first time. Left ventricular hemodynamic forces are less aligned to the main blood flow direction in patients compared to controls. Higher RV forces were seen along the pulmonary regurgitant and tricuspid inflow directions. Differences in forces versus

controls remain after pulmonary valve replacement suggesting that altered biventricular pumping does not normalize after surgery.

Keywords

Cardiac magnetic resonance imaging, four-dimensional flow, Pulmonary insufficiency, congenital heart disease, heart failure

Introduction

Patients with pulmonary regurgitation (PR) after repair of Tetralogy of Fallot (rToF) often develop dilatation of the right ventricle (RV) with progressive right ventricular dysfunction (4), decreased exercise capacity (18) and increased risk of ventricular arrhythmias and sudden death (14). Progressive RV dilatation and RV systolic dysfunction are the main current criteria for pulmonary valve replacement (PVR) to alleviate PR and decrease the risk of adverse outcomes (12, 16), (2). However, it is uncertain at what degree of dilatation intervention should be performed(4, 13). To better guide treatment, increased understanding of ventricular remodeling mechanisms and new quantitative measures of ventricular functional impairment after intervention are desirable.

Time-resolved three-dimensional velocity (4D flow) cardiac magnetic resonance imaging (MRI) offers a unique possibility to visualize and quantify intracardiac blood flow and has previously been used in patients with rToF to demonstrate disturbed kinetic energy in both ventricles (23). The 4D flow technique can also be used to quantify hemodynamic forces in the ventricles (1, 10, 11, 25), i.e. the force needed to accelerate the blood.

During systole the myocardium exerts a force to accelerate the blood and during diastole the blood decelerates, which leads to a counterforce in the myocardium (Newton's third law of motion). Patients with rToF have to accelerate a larger RV stroke volume (SV) than controls due to the pulmonary regurgitation volume and often present with right bundle branch block, which might further influence the intraventricular hemodynamic forces.

The hemodynamic forces in the RV have been studied in healthy volunteers and athletes showing a qualitative consistency between groups (1), but it has not been analyzed in patients with rToF.

The hemodynamic forces have also been shown to be disturbed in the left ventricle (LV) in patients with dilated cardiomyopathy and left bundle branch block (10, 11, 22). We therefore hypothesized that these disturbances in hemodynamic forces are related to increased wall stress and the development of remodeling also in the RV. Thus, hemodynamic forces may have the potential to help improve timing of PVR.

The aim of this study was therefore to quantify the hemodynamic forces in the RV and LV to further understand the pathophysiological mechanisms in patients with rToF and RV volume overload due to PR.

Materials and Methods

Study design

We prospectively included patients with rToF and PR > 20%, diagnosed by previous MRI or echocardiography and without pulmonary stenosis referred for MRI. A subset of patients (n=8) underwent PVR and a follow up MRI scan with 4D flow 6-12 months after surgery, performed using the same protocol and scanner as at baseline. Indications for PVR were PR fraction ≥35%, progressive RV dilatation with RV end-diastolic volume (EDV) ≥150 ml/m^2 and/or symptoms and signs of heart failure. Healthy controls (n=15) were recruited by advertising at the local institution. The controls underwent MRI including the same 4D flow sequence as used in patients. Inclusion criteria for controls were normal ECG and blood pressure <140/90 mmHg, no cardiovascular medication and no medical history of cardiovascular or other systemic disease.

The principles of the Helsinki declaration were followed, and the Regional Ethical Review Board in Lund, Sweden approved the study. Written informed consent was obtained from all subjects

before participation.

Cardiac Magnetic Resonance Imaging

Magnetic resonance images were acquired with the patient in the supine position using retrospective ECG gating, with a 1.5 T Achieva (Philips Healthcare, Best, the Netherlands) or a 1.5 T Magnetom Aera (Siemens Healthcare, Erlangen, Germany). The reason for using two different vendors was change of scanners at the hospital during the study.

Balanced steady-state free-precession (bSSFP) cine images covering the entire heart were acquired. Two-dimensional (2D) through-plane phase contrast (PC) flow measurements were performed in the ascending aorta in all subjects to quantify the effective stroke volume. In patients, flow in the pulmonary artery was also acquired to quantify the degree of PR and forward pulmonary flow during end-diastole was used to define restrictive RV physiology. On both scanners, validated (6, 17) prototype 4D-flow sequences for research purpose was used to quantify flow in a volume covering the whole heart. Typical imaging parameters are reported in Table 1. 4D-flow was accelerated with parallel imaging (SENSE 2x1 for Philips Achieva and GRAPPA 2x2 for Siemens Aera) and with a temporal segmentation factor (echo train length) of 2. Respiratory navigation for 4D flow was used in 7/18 patients, but due to long acquisition time no navigator was used in 11/18 patients. Gadolinium contrast was not given as part of the study protocol but 0.2 mmol/kg was administered in 16/18 patients due to clinical questions of myocardial fibrosis using late gadolinium enhancement (LGE).

Image analysis and calculation of hemodynamic forces

The Segment software package (http://segment.heiberg.se) was used for image analysis, with an in vitro and in vivo validated in-house developed module for 4D-flow analysis of hemodynamic forces (25). A validated method for first-order phase background correction (3, 5) and phase unwrapping (in case of high velocities in the right ventricular outflow tract (RVOT)) was performed prior to analysis.

Time-resolved delineations of the endocardium in RV and LV in all timeframes were manually drawn and end-diastolic volume (EDV), end-systolic volume (ESV) and SV were calculated. The delineations were transferred to the 4D-flow dataset. Based on the 4D-flow data the pressure gradient $\boldsymbol{g}$ (N) was calculated using the Navier-Stokes equation,

$$\boldsymbol{g} = -\rho\frac{\partial \boldsymbol{v}}{\partial t} - \rho(\boldsymbol{v} \cdot \nabla \boldsymbol{v}) + \mu\nabla^2\boldsymbol{v}$$

where $\boldsymbol{v}$ is the velocity (m/s), ρ the density of blood (1.05 g/cm^3) and μ the viscosity ($4.0 \cdot 10^{-3}$ Ns/m^2). The hemodynamic force was calculated for each time frame of the cardiac cycle by integrating the pressure gradients over the volume of the LV or RV respectively.

The hemodynamic force vectors were analyzed in three dimensions. To relate the forces to the anatomy of the heart and the main blood flow directions, a reference system based on the individual ventricle's anatomy was constructed as follows (Figure 1). First, the AV plane was defined in 2, 3 and 4 chamber views and the apical-basal direction was defined as perpendicular to the AV plane. The lateral-septal direction was defined as perpendicular to the apical-basal direction and parallel to the 3-chamber long-axis image plane and the AV plane. The inferior-anterior direction was defined as perpendicular to the other two directions. In the right ventricle the same directions were used, but the transversal directions were denoted septal-freewall and diaphragm-RVOT (right ventricular outflow tract).

158

159 *Analysis of hemodynamic forces*

160 Hemodynamic force data were resampled in time to a common reference heartbeat to display the
161 average force over time in patients and controls independent of different heart rates (Figure 2).

162 Root mean square (RMS) analysis was performed in all three directions to facilitate the
163 comparison between systolic and diastolic forces regardless of whether the force was negative or
164 positive in relation to the defined direction. RMS of hemodynamic forces was calculated
165 as $RMS = \sqrt{\frac{1}{N}\sum_{n=1}^{N} f_n^2}$, where N is the number of time frames in the cardiac cycle and f_n is the
166 force in the timeframe n.

167 The ratio between transversal (lateral-septal and inferior-anterior) and longitudinal (apical-basal)
168 forces was computed for the LV to analyze how the forces align with the blood flow. The
169 anatomy of the RV with inflow at an angle to the outflow prohibits a transverse/longitudinal ratio
170 to contribute to the understanding of force and flow alignment.

171 Hemodynamic forces are presented both without normalization ("absolute" values in Newton
172 (N)), and also indexed to ventricular volume to be able to compare forces independent of heart
173 size ("indexed" values in Newton/liter (N/l)).

174 The larger RV stroke volume compared to LV stroke volume results in larger variation of volume
175 of the RV during the cardiac cycle in rToF. This cause a larger motion of the ventricles compared
176 to controls and this may influence the measured hemodynamic forces (7, 24). To analyze how
177 much the potential difference in forces between patients and controls was explained by this
178 translational ventricular motion, the maximum center of volume motion of the left and right

ventricle were calculated for each force direction. The origin of center of volume was identified in enddiastole. The measured forces caused by the ventricular motion were calculated and presented as the proportion (%) of the intraventricular hemodynamic forces. LGE images were visually assessed where contrast enhancement in the RV wall, not including the septum, was considered RV fibrosis.

Statistical analyses

Statistical analyses were performed using GraphPad (v6.04, La Jolla, CA, USA). Continuous variables are presented as mean and standard deviation (SD) or median and range. Differences in characteristics, volumes and forces between rToF patients and healthy volunteers were assessed using the Mann-Whitney U test. Differences in forces before and after PVR were evaluated using the Wilcoxon Rank test. Associations between variables were analyzed by Spearman correlation. Results with a p-value <0.05 were considered statistically significant.

Results

Subject characteristics and volumetric data are summarized in Table 2. All patients had right bundle branch block. PR fraction was in 3/18 patients: 20-29%, 7/18 patients: 30-39% and 8/18 patients: ≥40%. Restrictive physiology was present in 13/18 patients. There were only minor tricuspid regurgitation, in one patient 18 % and in the remaining <10%. RV fibrosis was found in 13/18 patients, 2/18 had no RV fibrosis and in 2 patients LGE images were not acquired. Patients with rToF had higher heart rates, smaller LVEDV/BSA and higher RV volumes compared to

controls. A decrease in global function was seen predominantly for RVEF but LVEF was also lower compared to controls.

Qualitative hemodynamic force patterns

The mean hemodynamic force during the cardiac cycle in the three different directions are shown in Figure 2 for patients and controls. In early systole the forces were mainly directed towards the outflow tract and base of the heart in both LV and RV, reflecting the acceleration of blood out of the ventricles. In late systole the forces were reversed, corresponding to the deceleration of blood outflow during late systole. During the first part of early diastolic inflow the forces were directed towards the apex and diaphragm, reflecting acceleration of blood flowing into the ventricles. During the latter part of early diastolic inflow, the forces reversed and were mainly oriented towards the base, reflecting the deceleration of blood entering the ventricle. In patients with rToF and PR there was a continuous hemodynamic force throughout the diastole towards the base and RVOT (Figure 2, Panel C). This continuous RV hemodynamic force during diastole was not present in controls.

Quantitative hemodynamic forces - Left ventricle

Patients with rToF and PR had higher RMS of indexed hemodynamic forces in the LV both in systole and diastole in the lateral-septal/LVOT and inferior-anterior directions (Table 3A and Figure 3A and B). Higher absolute hemodynamic forces were found in patients in systole for the inferior-anterior and apical basal directions and in diastole for inferior-anterior direction.

The transversal hemodynamic forces in the LV (lateral-septal/LVOT and inferior-anterior) constitute a larger fraction of the total force during systole in patients with rToF compared to controls (Figure 4). The mean ratio of transversal and longitudinal (apical-basal) forces during systole was 1.03 (0.29) in rToF vs 0.72 (0.15) in controls (p=0.0007) and during diastole 0.49 (0.20) in rToF vs 0.44 (0.13) in controls (p=0.60).

Quantitative hemodynamic forces - Right ventricle

In systole, the absolute hemodynamic forces were larger in the diaphragm-RVOT and apical-basal directions in patients compared to controls. No differences were found between patients and controls for indexed hemodynamic forces during systole. In diastole, however, patients with rToF and PR had higher absolute and indexed hemodynamic forces in the diaphragm-RVOT and apical-basal directions (Table 3B, Figure 3C and 3D).

There was a moderate to strong positive correlation between PR fraction and RMS of hemodynamic forces in the diaphragm-RVOT direction (systole: r=0.59, p=0.01 and diastole: r=0.53, p=0.024). A strong correlation was also found for PR volume and hemodynamic forces in the diaphragm-RVOT direction (systole: r=0.74, p=0.0005; and diastole: r=0.65, p=0.0036).

Effect of PVR

Median follow up time after PVR was 10 months, range 6-21 months. One patient had a later reexamination than planned, 21 months after surgery, due to factors unrelated to the heart

condition. RV volumes decreased after surgery but RVEF and LV volumes and LVEF were unchanged (Table 4). After PVR patients still had lower LVEDV/BSA than controls, whereas RVESV and RVESV/BSA remained higher and RVEF lower (Table 2).

The effects of PVR on the individual patients' absolute hemodynamic forces are shown in Figure 5. To evaluate if the differences after surgery were only related to the change in volumes, the indexed hemodynamic forces are shown in Table 5A and B. The lower forces in the diaphragm-RVOT direction than controls remained also after indexing.

The intra-individual hemodynamic forces in the LV did not change after PVR (Figure 5), thus the ratio between transversal and longitudinal forces in the LV did not differ before compared to after PVR (systole p=0.64, diastole p=0.74). Patients with rToF after PVR still had higher forces in the inferior-anterior direction of the LV during both systole (0.39 N/ml (0.13)) and diastole (0.49 N/ml (0.18)) compared to controls (systole 0.23 N/ml (0.057), p=0.0011; diastole 0.18 N/ml (0.072), p<0.0001) (Figure 6). Patients also still had higher indexed LV hemodynamic forces after PVR in the lateral-septal/LVOT direction during systole compared to controls (1.13 N/ml (0.43) vs 0.65 N/ml (0.34), p=0.019).

Systolic RV hemodynamic forces in the diaphragm-RVOT direction decreased postoperatively (Figure 5 and Table 5B) resulting in lower forces postoperatively compared to controls (0.75 N/ml (0.17) vs 1.02 N/ml (0.29), p=0.0064). During diastole there was a decrease in the RMS of the hemodynamic forces in all directions; septal-freewall (p=0.0078), diaphragm-RVOT (p=0.0078) and apical-basal (p= 0.039) but patients with rToF still after PVR had higher forces in

the diaphragm-RVOT direction in diastole compared to controls (0.41 N/ml (0.11) vs 0.27 N/ml (0.12), p=0.046).

After PVR the higher LV indexed systolic hemodynamic forces in patients in the transversal planes compared to controls remained. The higher LV diastolic indexed hemodynamic forces in patients in the inferior-anterior direction compared to controls also remained after PVR and there was no difference in diastolic LV forces in the other directions.

In contrast to before PVR, the RV indexed systolic hemodynamic forces in the diaphragm-RVOT direction in patients was lower compared to controls after PVR. The higher indexed diastolic hemodynamic forces in the diaphragm-RVOT direction in patients compared to controls remained after PVR but the difference in the apical-basal direction no longer remained. Thus, alterations in hemodynamic forces remained after PVR.

Effect of translational ventricular movement on hemodynamic forces

The LV center of volume in patients moved more towards the septum/LVOT and inferiorly during the cardiac cycle than in controls (Table 6A). The proportion of the forces that was caused by LV center of volume motion varied from -14 % to +4 %, with no difference between patients and controls (Table 6B).

The RV center of volume had a larger movement towards the RV free wall, but less towards the septum and apex in patients compared to controls (Table 6A). The proportion of the forces that was caused by RV center of volume motion varied from -15 to +10 % (Table 6B). Differences between patients and controls were seen in the diaphragm-RVOT direction in diastole and the apical-basal direction in systole (Table 6A).

Discussion

This study is the first to quantify intracardiac hemodynamic forces in patients with rToF. The hemodynamic forces were less aligned with the intraventricular blood flow compared to controls in the LV. Higher forces in the RV are seen in patients along the regurgitant flow direction in the RVOT as well as tricuspid inflow. Forces remains altered after PVR indicating that the affected biventricular pumping does not normalize completely after surgery.

LV hemodynamic forces

The ratio between the transversal and longitudinal forces in the LV was higher in patients with rToF compared to controls, caused by both lower longitudinal forces and higher transversal forces in patients. This means that the main alignment of hemodynamic forces along the longitudinal axis seen in the healthy LV in controls (22) is altered in rToF patients with a small LV and preserved EF. This misalignment of force and flow has also been shown in patients with dilated cardiomyopathy and decreased EF (10). Ventricular dyssynchrony is thought to be one factor causing increased transversal vs. longitudinal hemodynamic forces in dilated cardiomyopathy (11) and might be a contributing factor also in patients with rToF.

The increased transversal forces suggest a less efficient LV pumping in patients, since these forces are not aligned with the blood flow. Earlier studies have suggested that the misalignment of intraventricular hemodynamic forces and blood flow activate epigenetic mechanisms leading to pathological cardiac remodeling, possibly through increased wall stress (20, 22). If this hypothesis is correct, one of the major purposes of PVR in patients with rToF and PR would be to

realign the hemodynamic forces in the ventricle with the blood flow. In this study LV forces did not change after surgery. This may indicate that the timing of surgery was not optimal and performed too late for completely normalizing blood flow and ventricular pumping.

A possible explanation to the higher forces in diastole could be that the LV in rToF has lower preload (19) and the LV has to generate higher forces to fill the ventricle, thereby accelerating the blood more. This is supported by our earlier study showing that patients with rToF have lower kinetic energy in systole, but no difference in diastole compared to controls (23).

RV hemodynamic forces

Increased RV hemodynamic forces were seen in the main flow directions in patients and was related to the increased flow volumes due to the pulmonary regurgitation. In diastole there were increased hemodynamic forces towards the RVOT. This can be explained by the continuous inflow to the RV due to the PR leading to a deceleration force in the opposite direction. This is supported by the correlation between PR volume and the hemodynamic forces towards the RVOT during diastole. In the control group there is no PR and thus no deceleration force towards the RVOT.

The increased force towards the base during diastole in patients compared to controls, both in absolute and indexed values, is the deceleration force on the inflowing blood from the tricuspid valve. Blood entering a healthy RV is mainly caused by longitudinal lengthening and this does not result in an acceleration of blood and thus no deceleration force (8). In patients with a PR, the systolic longitudinal shortening, and thus also diastolic lengthening, is decreased. As a result inflow of blood caused by radial pumping resulting in diastolic suction may be increased (24).

The radial pumping will result in a higher acceleration of blood flow entering the RV and may explain higher forces in the apical-basal direction in patients. Furthermore, diastolic function is decreased in rToF patients (15) and restrictive physiology has been linked to RV fibrosis in this patient group (21). In our patient group 72% of the patients with LGE data had RV fibrosis and 72% showed restrictive physiology. Further studies will show if diastolic dysfunction with or without RV fibrosis contribute to the higher forces in the apical-basal direction in patients with rToF.

Changes in hemodynamic forces in patients after PVR suggests that the decreased RV volume after surgery is the main cause of the decrease in RV hemodynamic forces. Surprisingly, the systolic diaphragm-RVOT force decreased to a level below the forces of the control population. We hypothesize that this may be explained by decreased myocardial contractility.

Effect of translational ventricular motion on hemodynamic forces

Translational ventricular motion contributes to the hemodynamic forces to equal extent in patients and controls except to RV systolic forces in the apical-basal direction and in RV diastolic forces in the diaphragm-RVOT direction. This translational contribution did not influence the interpretation of the results, as the magnitudes of differences were considerably larger than the magnitudes caused by motion of the ventricles. This result might seem unexpected considering that the LV in rToF patients have a larger net motion towards the RV in systole, but since the force depends on the acceleration and not only the distance traveled, the duration of the motion also important. Thus, translational motion of the ventricles is not likely to be a major confounder when calculating hemodynamic forces in future studies. Based on this the hemodynamic forces in this study are presented as the total force including the minor contribution caused be the motion of the ventricles to facilitate comparison with other studies.

Limitations

The study population is small, especially the subgroup after PVR. However, the control group showed results consistent with previous studies of hemodynamic forces in healthy subjects (1, 10). The larger RV stroke volume compared to LV stroke volume results in larger variation of volume of the RV during the cardiac cycle in rToF. This cause a larger motion of the ventricles compared to controls and this may influence the measured hemodynamic forces Intracardiac blood flow includes vortex formation, and in an ideal symmetric vortex the net vector would be zero, since the forces from either side of the vortex would each other cancel out. Therefore, the present hemodynamic force framework will not capture effects of symmetric vortices. However, the asymmetric anatomy of the heart typically leads to asymmetric vortices resulting in a net force.

Assessment of ventricular function must always be considered in the light of load-dependency and hemodynamic forces may also be dependent on pre-load and after-load. There are non-invasive load independent techniques described for left ventricular diastolic function (9) but to the best of our knowledge this has not been applied or validated in the right ventricle and especially not in patients with pulmonary regurgitation. Future studies might reveal if and how hemodynamic forces are load dependent.

There was a difference in heart rate between patients and controls and possible impact on hemodynamic forces cannot be ruled out. 4D flow was acquired both with and without respiratory gating, but the different methods have been shown to be comparable as shown by Kanski *et al* (17). MR scanners from two vendors were used in the study but a recent validation

study showed good agreement of hemodynamic forces between scans with and without respiratory gating and between different vendors (25). However, while agreement is generally good on a group basis, some variability remains. To minimize the potential effect of using two scanners in the study, the same scanner was always used before and after operation. Further, nine patients and nine controls were examined with the Philips scanner and nine patients and six controls with the Siemens scanner.

Conclusion

Patients with repaired Tetralogy of Fallot and pulmonary regurgitation have less alignment of hemodynamic forces and intraventricular blood flow in the left ventricle compared to controls. Higher right ventricular forces are seen in patients along the regurgitant flow direction in the right ventricular outflow tract and that of the tricuspid inflow direction. These altered force patterns remain after pulmonary valve replacement suggesting that the affected biventricular pumping does not normalize completely after surgery. The potential role of hemodynamic forces for treatment evaluation and decision making in rToF can be the aim for future studies.

Acknowledgements

Philips Healthcare is gratefully acknowledged for a research collaboration making the 4D-flow sequence available. We thank Siemens Healthcare for providing the 4D-flow sequence as the work-in-progress package WIP785K.

Grants

This work was funded by Swedish Heart–Lung foundation, Lund University, Skåne University Hospital, Region Skåne and Swedish Research Council. The funding bodies had no influence over study design, analysis, or data interpretation.

Disclosures

Einar Heiberg is stockholder and founder of Medviso AB that sells the Segment software for clinical use. Håkan Arheden is stockholder of Imacor AB, a core lab for medical image analysis. Marcus Carlsson has received consultancy fees from Imacor AB. The remaining authors have no competing interests.

References

1. **Arvidsson PM**, **Töger J**, **Carlsson M**, **Steding-Ehrenborg K**, **Pedrizzetti G**, **Heiberg E**, **Arheden H**. Left and right ventricular hemodynamic forces in healthy volunteers and elite athletes assessed with 4D flow magnetic resonance imaging. *Am J Physiol - Hear Circ Physiol* 312: H314–H328, 2017.

2. **Baumgartner H**, **Bonhoeffer P**, **De Groot NMS**, **De Haan F**, **Deanfield JE**, **Galie N**, **Gatzoulis MA**, **Gohlke-Baerwolf C**, **Kaemmerer H**, **Kilner P**, **Meijboom F**, **Mulder BJM**, **Oechslin E**, **Oliver JM**, **Serraf A**, **Szatmari A**, **Thaulow E**, **Vouhe PR**, **Walma E**, **Vahanian A**, **Auricchio A**, **Bax J**, **Ceconi C**, **Dean V**, **Filippatos G**, **Funck-Brentano C**, **Hobbs R**, **Kearney P**, **McDonagh T**, **Popescu BA**, **Reiner Z**, **Sechtem U**, **Sirnes PA**, **Tendera M**, **Vardas P**, **Widimsky P**, **Swan L**, **Andreotti F**, **Beghetti M**, **Borggrefe M**, **Bozio A**, **Brecker S**, **Budts W**, **Hess J**, **Hirsch R**, **Jondeau G**, **Kokkonen J**, **Kozelj M**, **Kucukoglu S**, **Laan M**, **Lionis C**, **Metreveli I**, **Moons P**, **Pieper PG**, **Pilossoff V**, **Popelova J**, **Price S**, **Roos-Hesselink J**, **Uva MS**, **Tornos P**, **Trindade PT**, **Ukkonen H**, **Walker H**, **Webb GD**, **Westby J**. ESC Guidelines for the management of grown-up congenital heart disease (new version 2010). *Eur Heart J* 31: 2915–2957, 2010.

3. **Bock J**, **Töger J**, **Bidhult S**, **Markenroth Bloch K**, **Arvidsson P**, **Kanski M**, **Arheden H**, **Testud F**, **Greiser A**, **Heiberg E**, **Carlsson M**. Validation and reproducibility of cardiovascular 4D-flow MRI from two vendors using 2x2 parallel imaging acceleration in pulsatile flow phantom and in vivo with and without respiratory gating. *Acta radiol.* (2018). doi: 10.1177/0284185118784981.

4. **Bokma JP**, **Winter MM**, **Oosterhof T**, **Vliegen HW**, **van Dijk AP**, **Hazekamp MG**,

Koolbergen DR, **Groenink M**, **Mulder BJ**, **Bouma BJ**. Preoperative thresholds for mid-to-late haemodynamic and clinical outcomes after pulmonary valve replacement in tetralogy of Fallot. *Eur Heart J* 37: 1–7, 2015.

5. **Busch J**, **Giese D**, **Kozerke S**. Image-based background phase error correction in 4D flow MRI revisited. *J Magn Reson Imaging* 46: 1516–1525, 2017.

6. **Carlsson M**, **Heiberg E**, **Toger J**, **Arheden H**. Quantification of left and right ventricular kinetic energy using four-dimensional intracardiac magnetic resonance imaging flow measurements. *Am J Physiol Heart Circ Physiol* 302: H893-900, 2012.

7. **Carlsson M**, **Rosengren A**, **Ugander M**, **Ekelund U**, **Cain PA**, **Arheden H**. Center of volume and total heart volume variation in healthy subjects and patients before and after coronary bypass surgery. *Clin Physiol Funct Imaging* 25: 226–233, 2005.

8. **Carlsson M**, **Ugander M**, **Heiberg E**, **Arheden H**. The quantitative relationship between longitudinal and radial function in left, right, and total heart pumping in humans. *Am J Physiol Heart Circ Physiol* 293: H636-44, 2007.

9. **Chung CS**, **Shmuylovich L**, **Kovács SJ**. What global diastolic function is, what it is not, and how to measure it. *Am J Physiol Circ Physiol* 309: H1392–H1406, 2015.

10. **Eriksson J**, **Bolger AF**, **Ebbers T**, **Carlhäll C-J**. Assessment of left ventricular hemodynamic forces in healthy subjects and patients with dilated cardiomyopathy using 4D flow MRI. *Physiol Rep* 4: e12685, 2016.

11. **Eriksson J**, **Zajac J**, **Alehagen U**, **Bolger AF**, **Ebbers T**, **Carlhäll C-J**. Left ventricular hemodynamic forces as a marker of mechanical dyssynchrony in heart failure patients with left bundle branch block. *Sci Rep* 7: 2971, 2017.

12. **Ferraz Cavalcanti PE**, **Sá MPBO**, **Santos CA**, **Esmeraldo IM**, **Escobar RR De**, **Menezes AM De**, **Azevedo OM De**, **Vasconcelos Silva FP De**, **Lins RFDA**, **Lima RDC**. Pulmonary valve replacement after operative repair of Tetralogy of Fallot: Meta-analysis and meta-regression of 3,118 patients from 48 studies. *J Am Coll Cardiol* 62: 2227–2243, 2013.

13. **Greutmann M**. Tetralogy of Fallot, pulmonary valve replacement, and right ventricular volumes: Are we chasing the right target? *Eur. Heart J.* 37 Oxford University Press: 836–839, 2016.

14. **Harrison DA**, **Harris L**, **Siu SC**, **MacLoghlin CJ**, **Connelly MS**, **Webb GD**, **Downar E**, **McLaughlin PR**, **Williams WG**. Sustained ventricular tachycardia in adult patients late after repair of tetralogy of Fallot. *J Am Coll Cardiol* 30: 1368–1373, 1997.

15. **Helbing WA**, **Niezen RA**, **Le Cessie S**, **van der Geest RJ**, **Ottenkamp J**, **de Roos A**. Right ventricular diastolic function in children with pulmonary regurgitation after repair of tetralogy of Fallot: volumetric evaluation by magnetic resonance velocity mapping. *J Am Coll Cardiol* 28: 1827–35, 1996.

16. **Heng EL**, **Gatzoulis MA**, **Uebing A**, **Sethia B**, **Uemura H**, **Smith GC**, **Diller G-PP**, **McCarthy KP**, **Ho SY**, **Li W**, **Wright P**, **Spadotto V**, **Kilner PJ**, **Oldershaw P**, **Pennell DJ**, **Shore DF**, **Babu-Narayan S V.** Immediate and Midterm Cardiac Remodeling After Surgical Pulmonary Valve Replacement in Adults With Repaired Tetralogy of Fallot: A Prospective Cardiovascular Magnetic Resonance and Clinical Study. *Circulation* 136: 1703–1713, 2017.

17. **Kanski M**, **Töger J**, **Steding-Ehrenborg K**, **Xanthis C**, **Bloch KM**, **Heiberg E**,

Carlsson M, **Arheden H**. Whole-heart four-dimensional flow can be acquired with preserved quality without respiratory gating, facilitating clinical use: a head-to-head comparison. *BMC Med Imaging* 15: 20, 2015.

18. **Kempny A**, **Dimopoulos K**, **Uebing A**, **Moceri P**, **Swan L**, **Gatzoulis MA**, **Diller G-P**. Reference values for exercise limitations among adults with congenital heart disease. Relation to activities of daily life--single centre experience and review of published data. *Eur Heart J* 33: 1386–1396, 2012.

19. **Kopic S**, **Stephensen SS**, **Heiberg E**, **Arheden H**, **Bonhoeffer P**, **Ersbøll M**, **Vejlstrup N**, **Søndergaard L**, **Carlsson M**. Isolated pulmonary regurgitation causes decreased right ventricular longitudinal function and compensatory increased septal pumping in a porcine model. *Acta Physiol* 221: 163–173, 2017.

20. **Mann DL**. Basic mechanisms of left ventricular remodeling: the contribution of wall stress. [Online]. *J Card Fail* 10: S202-6, 2004.

21. **Munkhammar P**, **Carlsson M**, **Arheden H**, **Pesonen E**. Restrictive right ventricular physiology after Tetralogy of Fallot repair is associated with fibrosis of the right ventricular outflow tract visualized on cardiac magnetic resonance imaging. *Eur Heart J Cardiovasc Imaging* 14: 978–985, 2013.

22. **Pedrizzetti G**, **Martiniello AR**, **Bianchi V**, **D 'onofrio A**, **Caso P**, **Tonti G**, **D'Onofrio A**, **Caso P**, **Tonti G**. Cardiac fluid dynamics anticipates heart adaptation. *J Biomech* 48: 388–391, 2015.

23. **Sjöberg P**, **Bidhult S**, **Bock J**, **Heiberg E**, **Arheden H**, **Gustafsson R**, **Nozohoor S**, **Carlsson M**. Disturbed left and right ventricular kinetic energy in patients with repaired

tetralogy of Fallot: pathophysiological insights using 4D-flow MRI. *Eur. Radiol.* (2018). doi: 10.1007/s00330-018-5385-3.

24. **Stephensen S**, **Steding-Ehrenborg K**, **Munkhammar P**, **Heiberg E**, **Arheden H**, **Carlsson M**. The relationship between longitudinal, lateral, and septal contribution to stroke volume in patients with pulmonary regurgitation and healthy volunteers. *Am J Physiol Heart Circ Physiol* 306: H895-903, 2014.

25. **Töger J**, **Arvidsson PM**, **Bock J**, **Kanski M**, **Pedrizzetti G**, **Carlsson M**, **Arheden H**, **Heiberg E**. Hemodynamic forces in the left and right ventricles of the human heart using 4D flow magnetic resonance imaging: Phantom validation, reproducibility, sensitivity to respiratory gating and free analysis software. *PLoS One* 13, 2018.

Figure Captions

Figure 1. Spatial reference for hemodynamic forces. A: The atrioventricular (AV) plane was defined in the 2-, 3- and 4-chamber view. B: The apical-basal direction was perpendicular to the AV plane. C: The lateral-septal direction was parallel to the AV plane (perpendicular to the apical-basal direction) and parallel to the 3-chamber long-axis image plane. The inferior-anterior direction was defined as perpendicular to both the apical-basal and lateral-septal planes. D: In the right ventricle the same directions were used, but the transversal directions were renamed septal-freewall and diaphragm-RVOT (right ventricular outflow tract).

Figure 2. Mean hemodynamic forces with 95% CI during the cardiac cycle in patients with repaired Tetralogy of Fallot and pulmonary regurgitation (rToF) (A and C) and controls (B and D). A and B shows data for the left ventricle (LV) and C and D shows the right ventricle (RV). In the LV the hemodynamic forces are mainly directed towards the septum/LVOT and the base when the blood is accelerated during systole and towards the base in diastole when blood entering the ventricle is decelerated. In the RV the hemodynamic forces are mainly directed towards the RVOT and base during systole reflecting the acceleration of the blood and during diastole towards the base due to the deceleration of the blood entering though the tricuspid valve, but in patients with rToF there is also a decelerating force towards the RVOT due to the pulmonary regurgitation volume.

Figure 3. RMS of hemodynamic forces indexed to ventricular volume in patients with repaired Tetralogy of Fallot and pulmonary regurgitation (rToF) and controls. A and B shows the left

ventricle (LV), C and D shows the right ventricle (RV). Systolic hemodynamic forces are shown in the left column and diastolic in the right column. Values are presented as mean (SD).

In the LV patients with rToF and pulmonary regurgitation (PR) had higher hemodynamic forces in the lateral-septal/LVOT direction and the inferior anterior direction, thus acting un-aligned with the blood flow, than controls in both systole and diastole.

In the RV there was no difference between patients with rToF and pulmonary regurgitation and controls in systole. However, in diastole patients had higher decelerating forces on the blood flow from the PR (RVOT direction) and tricuspid valve (basal direction).

Figure 4. Transversal/longitudinal ratio of hemodynamic forces in the LV of patients with repaired Tetralogy of Fallot and pulmonary regurgitation (rToF) and controls. Panel A shows systolic values where patients had higher ratio than controls. Panel B shows diastolic values where there was no difference between the groups.

Figure 5. RMS of hemodynamic forces in patients with repaired Tetralogy of Fallot and pulmonary regurgitation (rToF) before and after pulmonary valve replacement (PVR). Values are presented as mean (SD).

There was no difference in hemodynamic forces in the left ventricle (LV) after surgery compared to before. Panel A shows LV forces in systole and Panel B LV forces in diastole.

Right ventricular (RV) systolic forces decreased in the diaphragm-RVOT direction, Panel C. There was a decrease in RV forces in all three directions during diastole, Panel D.

Figure 6. RMS of hemodynamic forces in patients with repaired Tetralogy of Fallot (rToF) after pulmonary valve replacement (PVR) compared to controls. Values are presented as mean (SD).

Patients after pulmonary valve replacement (PVR) had higher systolic left ventricular (LV) forces in the transversal directions (inferior-anterior and lateral-septal/LVOT) and higher diastolic LV forces in the inferior-anterior direction, compared to controls, Panel A.

Patients after PVR had lower systolic RV forces, but higher RV diastolic forces in the diaphragm-RVOT direction compared to controls.

Text tables

Table 1. Imaging parameters used in the current study

Siemens 1.5 T MAGNETOM Aera			
Sequence parameters	**bSSFP CINE**	**2D Flow**	**4D Flow**
Flip angle [°]	70	20	8
TE/TR [ms]	1.2/2.7	2.7/4.9	3.5/5.6
Slice thickness [mm]	8	5	Not applicable
Slice gap [mm]	0	Not applicable	Not applicable
Reconstructed spatial resolution [mm^3]	1.2x1.2x8	1.6x1.6x5	3x3x3
Acquired temporal resolution [ms]	43	29	45
Reconstructed timephases	25	35	40
Gating method	Retrospective ECG	Retrospective ECG	Retrospective ECG
Velocity encoding (VENC) [cm/s]	Not applicable	200	100
Philips 1.5 T Achieva			
Sequence parameters	**bSSFP CINE**	**2D Flow**	**4D Flow**
Flip angle [°]	60	15	8
TE/TR [ms]	1.4/2.8	3.0/5.2	3.7/6.3
Slice thickness [mm]	8	6	Not applicable
Slice gap [mm]	0	Not applicable	Not applicable
Reconstructed spatial resolution [mm^3]	1.4x1.4x8	1.2x1.2x6	3x3x3
Acquired temporal resolution [ms]	47	29	50
Reconstructed timephases	30	35	40
Gating method	Retrospective ECG	Retrospective ECG	Retrospective ECG
Velocity encoding (VENC) [cm/s]	Not applicable	200	100

bSSFP, balanced steady-state free-precession; 2D, 2-dimensional; 4D, 4-dimensional; TE, echo time; TR, repetition time

566

567 **Table 2**. Characteristics and volumetric measurements in patients with repaired tetralogy of

568 Fallot and pulmonary regurgitation before and after pulmonary valve replacement and controls.

569 Values are presented as mean (SD).

Mean (SD)	**Patients with rToF before PVR** (n=18)	**Controls** (n=15)	**P-value** rToF before PVR vs Controls	**Patients with rToF after PVR** (n=8)	**P-value** rToF after PVR vs Controls
Age (years)	29 (13)	31 (7)	0.13	36 (14)	0.65
Gender (male/female)	11/7	10/5	n/a	6/2	n/a
HR (bpm) at 4D flow acquisition	71 (9)	60 (8)	0.0018	73 (12)	0.0099
BSA (m^2)	1.9 (0.2)	1.9 (0.2)	0.78	2.0 (0.2)	0.46
LVEDV (ml)	155 (26)	172 (36)	0.11	155 (24)	0.27
LVEDV/BSA (ml/m^2)	82 (11)	91 (14)	0.024	78 (13)	0.017
LVESV (ml)	72 (16)	70 (17)	0.78	64 (13)	0.52
LVESV/BSA (ml/m^2)	38 (7)	37 (8)	0.92	32 (6)	0.18
LVEF (%)	54 (6)	60 (6)	0.035	59 (4)	0.69
RVEDV (ml)	291 (67)	192 (41)	<0.0001	228 (40)	0.067
RVEDV/BSA (ml/m^2)	153 (24)	101 (13)	<0.0001	114 (19)	0.075
RVESV (ml)	167 (49)	88 (23)	<0.0001	140 (32)	0.0002
RVESV/BSA (ml/m^2)	87 (19)	46 (9)	<0.0001	70 (15)	<0.0001
RVEF (%)	43 (6)	55 (6)	<0.0001	39 (5)	<0.0001
PRF (%)	39 (9)	0	<0.0001	0	n/a

570 rToF, repaired Tetralogy of Fallot; PVR, pulmonary valve replacement; HR, heart rate; BSA,

571 Body Surface Area; LVEDV, left ventricular end-diastolic volume; LVESV, left ventricular end-

572 systolic volume; LVEF, left ventricular ejection fraction; RVEDV, right ventricular end-diastolic

573 volume; RVESV, right ventricular end-systolic volume; RVEF; right ventricular ejection

574 fraction; PRF, pulmonary regurgitation fraction

Table 3A: RMS of hemodynamic force in the left ventricle for patients with repaired Tetralogy of Fallot and pulmonary regurgitation (rToF) and controls in N and N/l. Values are presented as mean (SD).

Force direction Mean (SD)		**Systole**			**Diastole**		
		rToF (n=18)	**Controls (n=15)**	**P-value**	**rToF (n=18)**	**Controls (n=15)**	**P-value**
Lateral-septal/LVOT	N	0.12 (0.034)	0.098 (0.047)	0.12	0.041 (0.016)	0.033 (0.016)	0.10
	N/l	1.05 (0.44)	0.65 (0.34)	0.011	0.37 (0.15)	0.23 (0.064)	0.0031
Inferior-anterior	N	0.046 (0.029)	0.028 (0.0084)	0.0022	0.045 (0.016)	0.024 (0.012)	0.0005
	N/l	0.43 (0.16)	0.23 (0.057)	<0.0001	0.43 (0.15)	0.18 (0.072)	<0.0001
Apical-basal	N	0.13 (0.035)	0.18 (0.062)	0.025	0.14 (0.045)	0.13 (0.037)	0.56
	N/l	1.16 (0.46)	1.24 (0.42)	0.42	1.19 (0.38)	0.87 (0.17)	0.0075

rToF, repaired Tetralogy of Fallot; LVOT, left ventricular outflow tract

579 **Table 3B**: RMS of hemodynamic force in the right ventricle for patients with repaired Tetralogy of Fallot and pulmonary regurgitation

580 (rToF) and controls in N and N/l. Values are presented as mean (SD).

Force direction Mean (SD)		**Systole**			**Diastole**		
		rToF (n=18)	**Controls (n=15)**	**P-value**	**rToF (n=18)**	**Controls (n=15)**	**P-value**
Septal-freewall	N	0.079 (0.039)	0.058 (0.019)	0.18	0.058 (0.025)	0.042 (0.012)	0.14
	N/l	0.38 (0.19)	0.40 (0.12)	0.46	0.29 (0.093)	0.29 (0.13)	0.84
Diaphragm-RVOT	N	0.25 (0.089)	0.17 (0.059)	0.0075	0.11 (0.048)	0.040 (0.015)	<0.0001
	N/l	1.04 (0.32)	1.02 (0.29)	0.92	0.52 (0.19)	0.27 (0.12)	<0.0001
Apical-basal	N	0.19 (0.096)	0.13 (0.055)	0.040	0.15 (0.071)	0.079 (0.030)	0.0001
	N/l	0.87 (0.45)	0.79 (0.31)	0.70	0.71 (0.24)	0.49 (0.14)	0.0017

581 rToF, repaired Tetralogy of Fallot; RVOT, right ventricular outflow tract

582

583

584 **Table 4.** Volumetric measurements in patients with repaired Tetralogy of Fallot (rToF) before

585 and after pulmonary valve replacement. Values are presented as mean (SD).

Mean (SD) (n=8)	**Before PVR**	**After PVR**	**P=value**
Left ventricle			
LVEDV (ml)	152 (26)	155 (24)	0.46
LVEDV/BSA (ml/m^2)	77 (10)	78 (13)	0.55
LVESV (ml)	71 (17)	64 (13)	0.20
LVESV/BSA (ml/m^2)	36 (7)	32 (6)	0.20
LVEF (%)	53 (7)	59 (4)	0.11
Right ventricle			
RVEDV (ml)	327 (57)	228 (40)	0.0078
RVEDV/BSA (ml/m^2)	165 (17)	114 (19)	0.0078
RVESV (ml)	192 (43)	140 (32)	0.016
RVESV/BSA (ml/m^2)	97 (13)	70 (15)	0.016
RVEF (%)	42 (5)	39 (5)	0.15

586 PVR, pulmonary valve replacement; LVEDV, left ventricular end-diastolic volume; LVESV, left

587 ventricular end-systolic volume; LVEF, left ventricular ejection fraction; RVEDV, right

588 ventricular end-diastolic volume; RVESV, right ventricular end-systolic volume; RVEF; right

589 ventricular ejection fraction

590

Table 5A: RMS of hemodynamic force in the left ventricle for patients with repaired Tetralogy of Fallot and pulmonary regurgitation (rToF) before and after pulmonary valve replacement in N and N/l. Values are presented as mean (SD).

Force direction Mean (SD), n=8		**Systole**			**Diastole**		
		Before PVR	**After PVR**	**P-value**	**Before PVR**	**After PVR**	**P-value**
Lateral-septal/LVOT	N	0.13 (0.046)	0.13 (0.046)	0.64	0.039 (0.015)	0.035 (0.014)	0.31
	N/l	1.11 (0.63)	1.13 (0.43)	0.84	0.40 (0.17)	0.32 (0.13)	0.11
Inferior-anterior	N	0.050 (0.041)	0.040 (0.011)	0.84	0.045 (0.016)	0.040 (0.011)	0.38
	N/l	0.45 (0.22)	0.39 (0.13)	0.46	0.49 (0.18)	0.43 (0.14)	0.15
Apical-basal	N	0.14 (0.037)	0.15 (0.028)	0.55	0.12 (0.044)	0.12 (0.044)	0.55
	N/l	1.28 (0.62)	1.34 (0.32)	0.64	1.06 (0.44)	1.20 (0.44)	0.38

PVR, pulmonary valve replacement; LVOT, left ventricular outflow tract

Table 5B: RMS of hemodynamic force (SD) in the right ventricle for patients with repaired Tetralogy of Fallot and pulmonary regurgitation (rToF) before and after pulmonary valve replacement in N and N/l. Values are presented as mean (SD).

Force direction Mean (SD), n=8		**Systole**			**Diastole**		
		Before PVR	**After PVR**	**P-value**	**Before PVR**	**After PVR**	**P-value**
Septal-freewall	N	0.087 (0.047)	0.071 (0.035)	0.38	0.067 (0.023)	0.043 (0.011)	0.0078
	N/l	0.35 (0.22)	0.32 (0.14)	0.64	0.30 (0.097)	0.29 (0.093)	0.74
Diaphragm-RVOT	N	0.30 (0.10)	0.13 (0.060)	0.0078	0.13 (0.052)	0.063 (0.013)	0.0078
	N/l	1.12 (0.46)	0.75 (0.17)	0.039	0.58 (0.22)	0.41 (0.11)	0.016
Apical-basal	N	0.20 (0.12)	0.13 (0.047)	0.039	0.18 (0.095)	0.11 (0.41)	0.039
	N/l	0.80 (0.50)	0.65 (0.19)	0.74	0.70 (0.33)	0.64 (0.27)	0.84

PVR, pulmonary valve replacement; RVOT, right ventricular outflow tract

Table 6A. Maximum center of volume motion of the left and right ventricle during the cardiac cycle. The three directions applied for the calculations have been divided in their two opposite directions for separate values from the origin of center of volume in enddiastole. Values are presented as mean distance in mm (SD).

	Force direction Mean (SD), mm	**rToF (n=18)**	**Controls (n=15)**	**P-value**
Left Ventricle	**Lateral**	0.9 (0.9)	1.0 (0.5)	0.13
	Septal/LVOT	4.4 (1.5)	1.4 (0.9)	<0.0001
	Inferior	4.0 (1.5)	1.9 (0.9)	0.0007
	Anterior	0.9 (0.9)	0.9 (0.5)	0.46
	Basal	1.0 (1.2)	1.1 (2.3)	0.61
	Apical	5.2 (2.5)	5.1 (2.0)	0.82
Right Ventricle	**Freewall**	2.6 (1.7)	0.2 (0.3)	<0.0001
	Septal	0.8 (0.7)	3.0 (1.2)	<0.0001
	Diaphragm	1.3 (1.4)	0.9 (0.8)	0.54
	RVOT	4.1 (2.5)	4.3 (2.6)	0.82
	Basal	1.4 (1.0)	0.3 (0.5)	0.0006
	Apical	3.4 (2.1)	9.8 (2.9)	<0.0001

rToF, repaired Tetralogy of Fallot; LVOT, left ventricular outflow tract; RVOT, right ventricular outflow tract

Table 6B. Proportion (%) of the calculated hemodynamic forces caused by the center of volume motion of the left and right ventricle. Values are presented as mean (SD).

	Force direction Mean (SD)	**Systole**			**Diastole**		
		rToF	**Controls**	**P-value**	**rToF**	**Controls**	**P-value**
Left Ventricle	**Lateral-septal/LVOT**	-8 (6)	-7 (8)	0.76	-11 (8)	-9 (14)	0.65
	Inferior-anterior	-14 (16)	-13 (16)	0.68	-9 (12)	-13 (20)	0.63
	Apical-basal	-1 (9)	-4 (11)	0.55	4 (9)	4 (12)	0.94
Right Ventricle	**Septal-freewall**	-5 (16)	-3 (17)	0.88	-15 (11)	-15 (14)	0.85
	Diaphragm-RVOT	9 (7)	10 (11)	0.77	6 (11)	-9 (11)	0.0024
	Apical-basal	0 (5)	6 (16)	0.0078	-6 (10)	-9 (18)	0.55

rToF, repaired Tetralogy of Fallot; LVOT, left ventricular outflow tract; RVOT, right ventricular outflow tract

610 **Figure 1**

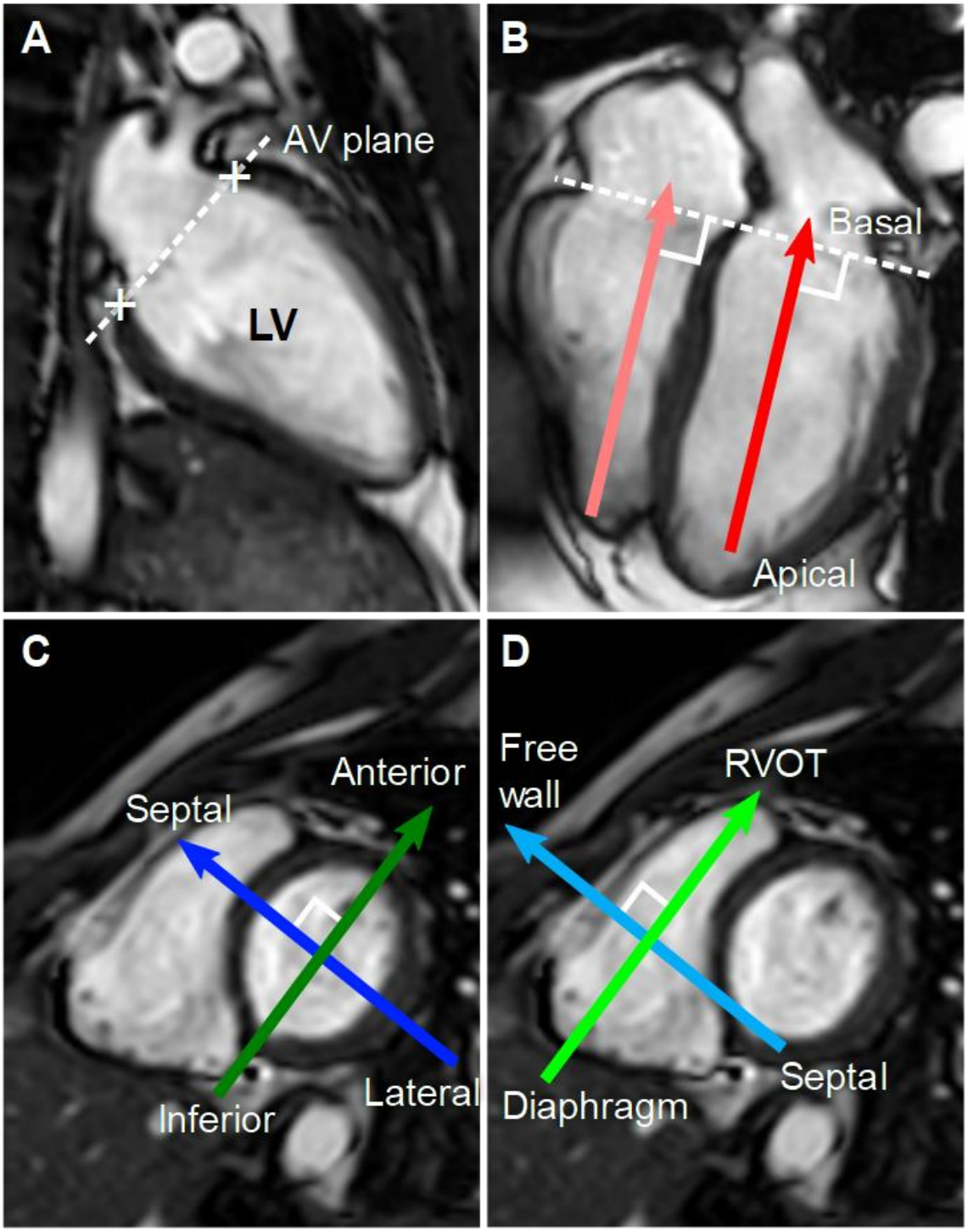

611

Figure 2

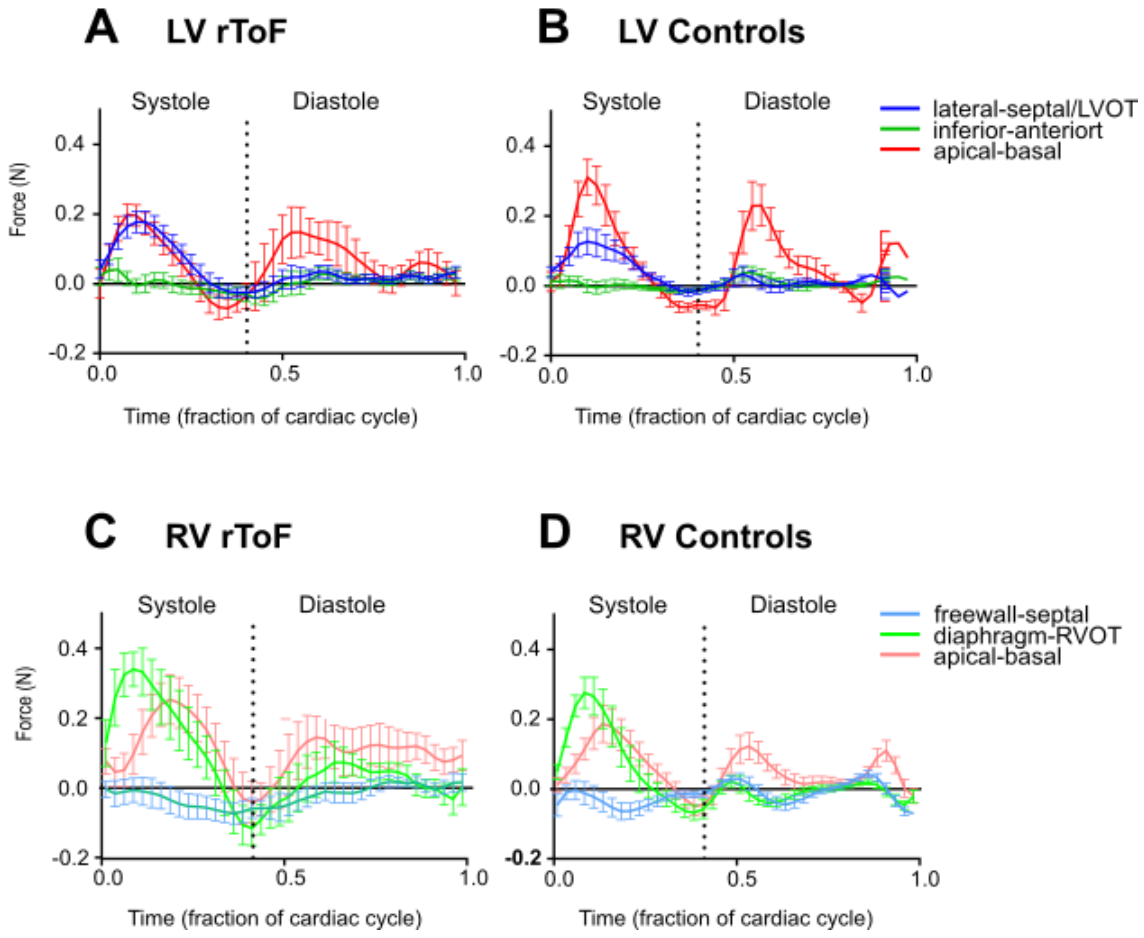
A
LV rToF
B
LV Controls
Systole
Diastole
Force (N)
0.4
0.2
0.0
-0.2
0.0
0.5
1.0
Time (fraction of cardiac cycle)
lateral-septal/LVOT
inferior-anteriort
apical-basal
C
RV rToF
D
RV Controls
freewall-septal
diaphragm-RVOT
apical-basal

Figure 3

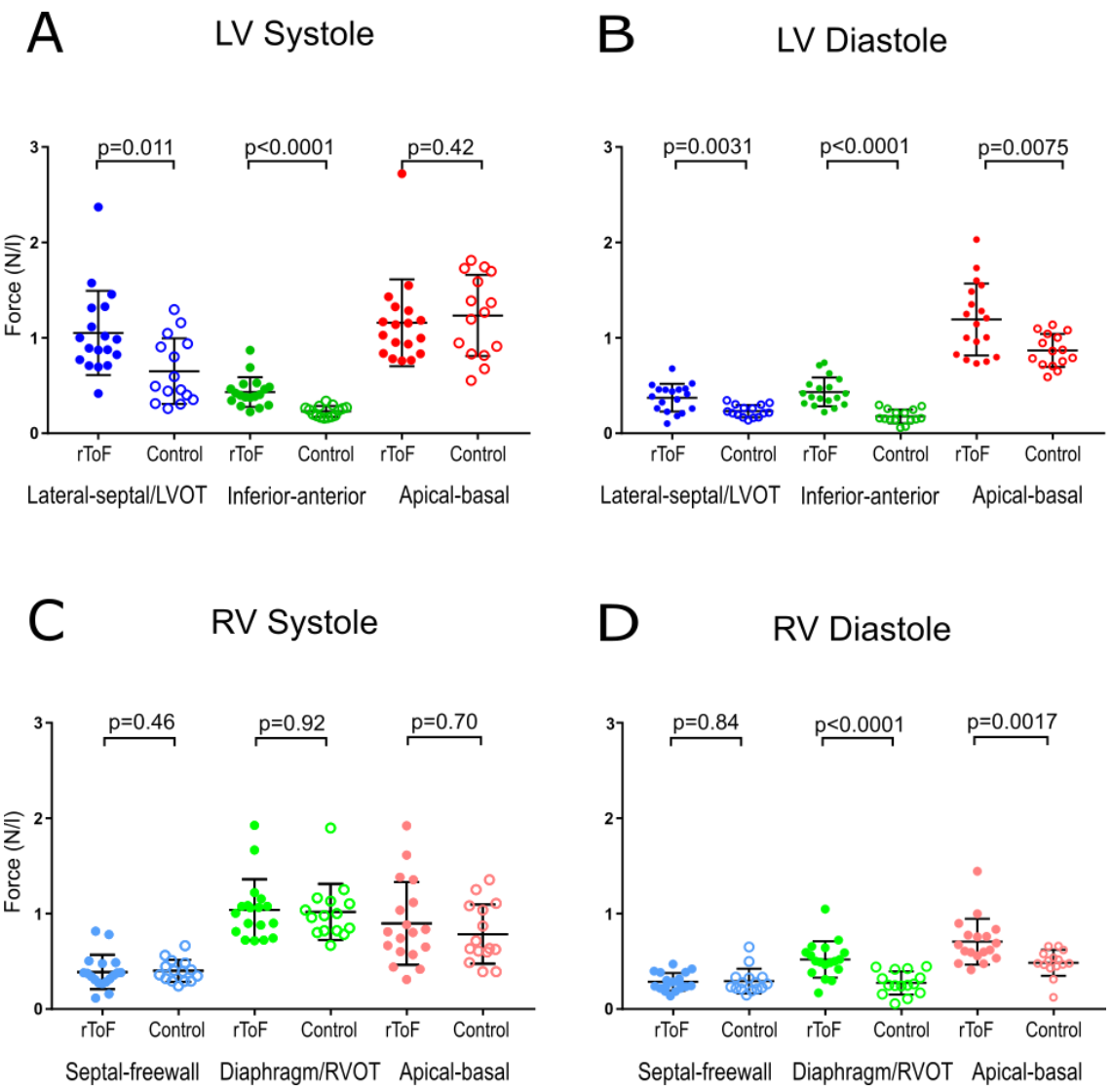
A
LV Systole
p=0.011
p<0.0001
p=0.42
Force (N/I)
rToF
Control
Lateral-septal/LVOT
Inferior-anterior
Apical-basal
B
LV Diastole
p=0.0031
p<0.0001
p=0.0075
C
RV Systole
p=0.46
p=0.92
p=0.70
Septal-freewall
Diaphragm/RVOT
D
RV Diastole
p=0.84
p<0.0001
p=0.0017

Figure 4

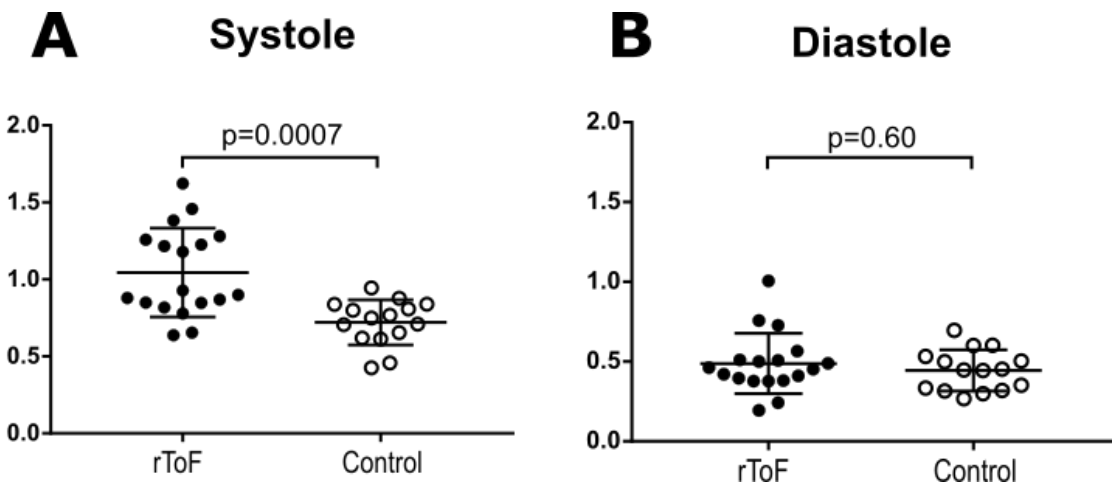
A
Systole
p=0.0007
2.0
1.5
1.0
0.5
0.0
rToF
Control
B
Diastole
p=0.60
2.0
1.5
1.0
0.5
0.0
rToF
Control

Figure 5

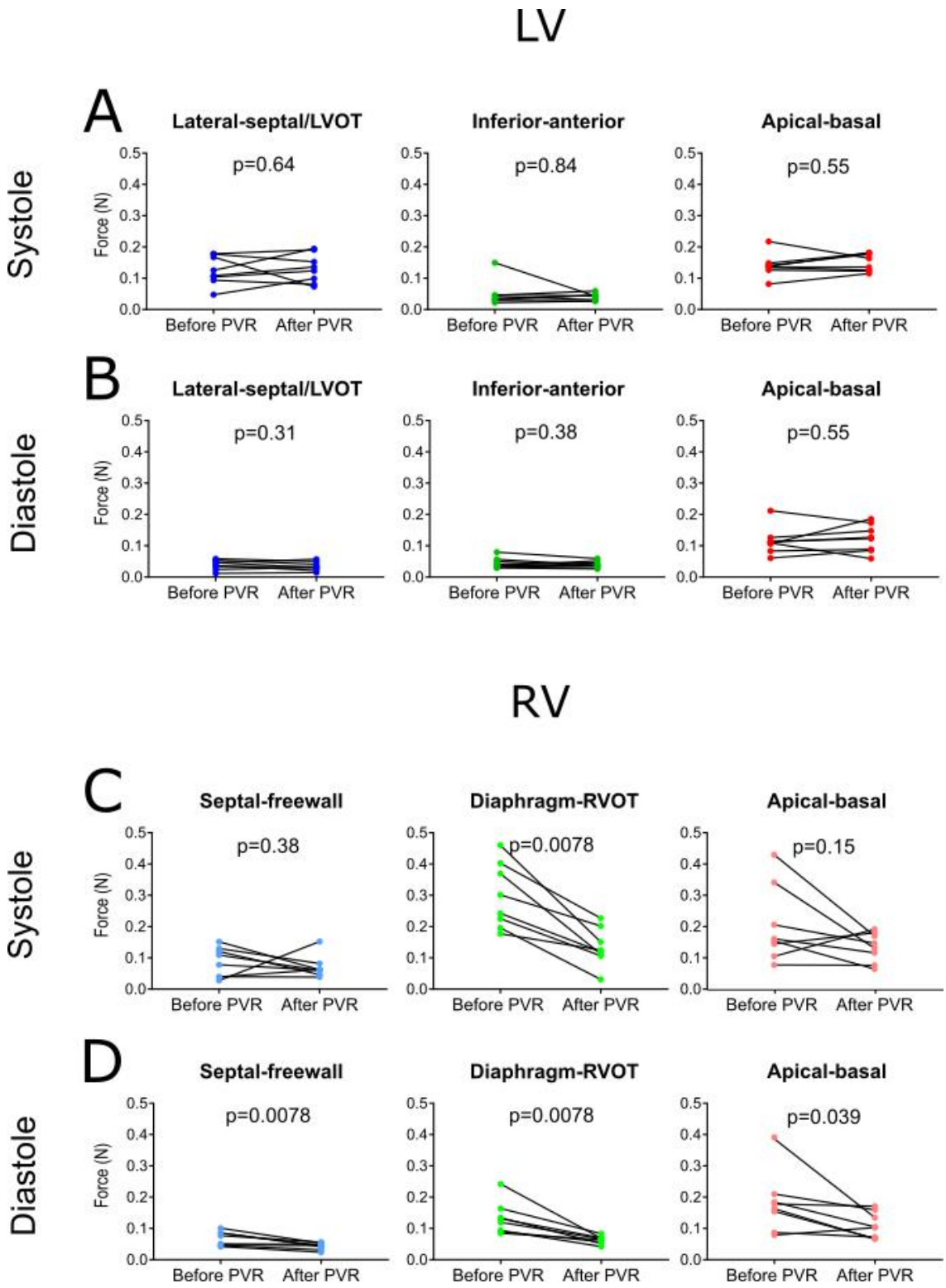
LV
A
Lateral-septal/LVOT
Inferior-anterior
Apical-basal
Systole
p=0.64
p=0.84
p=0.55
B
Diastole
p=0.31
p=0.38
p=0.55
RV
C
Septal-freewall
Diaphragm-RVOT
Apical-basal
p=0.38
p=0.0078
p=0.15
D
p=0.0078
p=0.0078
p=0.039
Force (N)
Before PVR
After PVR

Figure 6

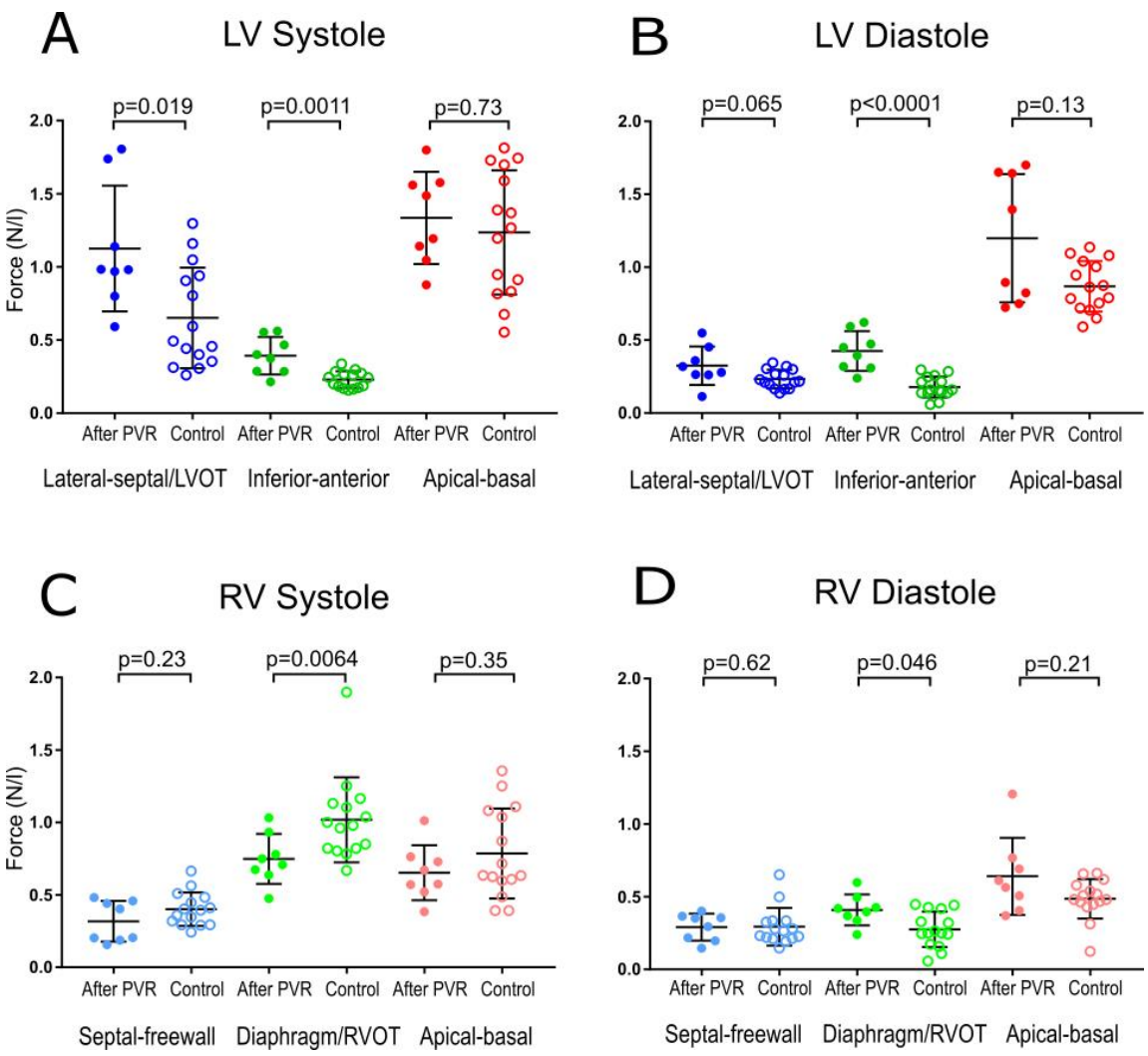
A
LV Systole
p=0.019
p=0.0011
p=0.73
Force (N/I)
2.0
1.5
1.0
0.5
0.0
After PVR
Control
After PVR
Control
After PVR
Control
Lateral-septal/LVOT
Inferior-anterior
Apical-basal
B
LV Diastole
p=0.065
p<0.0001
p=0.13
After PVR
Control
After PVR
Control
After PVR
Control
Lateral-septal/LVOT
Inferior-anterior
Apical-basal
C
RV Systole
p=0.23
p=0.0064
p=0.35
Force (N/I)
After PVR
Control
After PVR
Control
After PVR
Control
Septal-freewall
Diaphragm/RVOT
Apical-basal
D
RV Diastole
p=0.62
p=0.046
p=0.21
After PVR
Control
After PVR
Control
After PVR
Control
Septal-freewall
Diaphragm/RVOT
Apical-basal